Interplay of RsbM and RsbK controls the σ^B activity of *Bacillus cereus*

Lei-Chin Chen,[1†] Jung-Chi Chen,[2†] Jwu-Ching Shu,[3] Chien-Yen Chen,[4] Ssu-Ching Chen,[5] Shu-Hwa Chen,[6] Chun-Yen Lin,[7] Chi-Yu Lu[8] and Chien-Cheng Chen[2*]

[1]*Department of Nutrition, I-Shou University, no. 8, Yida Rd., Jiaosu Village, Yanchao District, Kaohsiung 82445, Taiwan.*

[2]*Department of Biotechnology, National Kaohsiung Normal University, 62 Shenjhong Rd., Yanchao District, Kaohsiung 82444, Taiwan.*

[3]*Department of Medical Biotechnology and Laboratory Science, Chang Gung University, Wen-Hwa 1st Road, Kwei-Shan, Tao-Yuan County 333, Taiwan.*

[4]*Department of Earth and Environmental Sciences, National Chung Cheng University, 168 University Road, Min-Hsiung, Chiayi 621, Taiwan.*

[5]*Department of Life Sciences, National Central University, no. 300, Jhongda Rd., Jhongli City, Taoyuan 32001, Taiwan.*

[6]*Computational Biology Research Center, Advanced Industrial Science and Technology, Japan.*

[7]*Institute of Information Science, Academia Sinica, Taipei, Taiwan.*

[8]*Department of Biochemistry, College of Medicine, Kaohsiung Medical University, Kaohsiung 80708, Taiwan.*

Summary

The alternative transcription factor σ^B of *Bacillus cereus* controls the expression of a number of genes that respond to environmental stress. Four proteins encoded in the *sigB* gene cluster, including RsbV, RsbW, RsbY (RsbU) and RsbK, are known to be essential in the σ^B-mediated stress response. In the context of stress, the hybrid sensor kinase RsbK is thought to phosphorylate the response regulator RsbY, a PP2C serine phosphatase, leading to the dephosphorylation of the phosphorylated RsbV. The unphosphorylated RsbV then sequesters the σ^B antagonist, RsbW, ultimately liberating σ^B. The gene arrangement reveals an open reading frame, *bc1007*, flanked immediately downstream by *rsbK* within the *sigB* gene cluster. However, little is known about the function of *bc1007*. In this study, the deletion of *bc1007* resulted in high constitutive σ^B expression independent of environmental stimuli, indicating that *bc1007* plays a role in σ^B regulation. A bacterial two-hybrid analysis demonstrated that BC1007 interacts directly with RsbK, and autoradiographic studies revealed a specific C^{14}-methyl transfer from the radiolabelled S-adenosylmethionine to RsbK when RsbK was incubated with purified BC1007. Our data suggest that BC1007 (RsbM) negatively regulates σ^B activity by methylating RsbK. Additionally, mutagenic substitution was employed to modify 12 predicted methylation residues in RsbK. Certain RsbK mutants were able to rescue σ^B activation in a *rsbK*-deleted bacterial strain, but RsbK$_{E439A}$ failed to activate σ^B, and RsbK$_{E446A}$ only moderately induced σ^B. These results suggest that Glu439 is the preferred methylation site and that Glu446 is potentially a minor methylation site. Gene arrays of the *rsbK* orthologues and the neighbouring *rsbM* orthologues are found in a wide range of bacteria. The regulation of sigma factors through metylation of RsbK-like sensor kinases appears to be widespread in the microbial world.

Introduction

Bacillus cereus is a gram-positive, facultatively anaerobic, spore-forming bacterium that produces a large number of virulence factors that can either cause food-borne illnesses with emetic and diarrhoeal symptoms or promote opportunistic infections (Agata *et al.*, 1996; Ehling-Schulz *et al.*, 2004; Schoeni and Wong, 2005). In the context of food processing or host immune pressure, the bacterial stress response is a major determinant of bacterial cell survival and growth (Mihaljevic *et al.*, 2007; Zotta *et al.*, 2008). A range of alternative bacterial transcription factors with distinct promoter specificities can confer resistance to multiple stressors by controlling the transcription of different regulons (Missiakas and Raina, 1998; Gruber and Gross, 2003; Kazmierczak *et al.*, 2005). The alternative transcription factor σ^B of *B. cereus* governs the transcription of σ^B-dependent genes and enables the cells to counteract fluctuations in temperature, pH or osmolarity (Price, 2002; Hecker *et al.*, 2007).

σ[B] is regulated by a partner-switching mechanism that has been extensively studied in *Bacillus subtilis*. RsbV and RsbW comprise the basic core proteins of σ[B] regulation, and they participate in protein–protein interactions and/or the mechanisms of serine/threonine phosphorylation. In unstressed cells, σ[B] is kept inactive by sequestration in a protein complex with the anti-sigma factor RsbW, which prevents σ[B] from associating with the core RNA polymerase (Alper *et al.*, 1996; Voelker *et al.*, 1996; Delumeau *et al.*, 2002). RsbW is a bi-functional protein that also acts as a kinase and can phosphorylate the anti-anti-sigma factor RsbV. Phosphorylated RsbV does not have the capability to sequester RsbW. When under conditions of stress, two serine/threonine protein phosphatases, RsbP and RsbU, catalyse the dephosphorylation of phosphorylated RsbV, and the unphosphorylated RsbV then forms an alternative complex with RsbW, thereby allowing σ[B] to bind to RNA polymerase.

In contrast to the regulatory strategy of partner-switching mechanisms, the two-component signal transduction system (TCS) is a common regulation module in bacteria for environmental adaptation, such as the induction of virulence factors, the formation of biofilms, the initiation of sporulation, chemotaxis, quorum sensing, and the utilization of nutrients (Hoch and Silhavy, 1995; Stock *et al.*, 2000; Galperin, 2006). Typical TCSs are comprised of a sensor and a response regulator (RR). Upon receiving environmental stimuli, the sensor initiates autophosphorylation of a conserved histidine residue in the H-box and transfers the phosphate to the downstream RR by direct phosphoryl transfer or through a more complex, multi-step His-Asp-His-Asp transfer via the histidine-containing phosphotransferase (Hpt) protein (Hoch and Silhavy, 1995; Stock *et al.*, 2000; Bijlsma and Groisman, 2003). In most cases, the phosphorylation of the RR receiver (REC) domain can modulate the function of the coupled output domain (Hoch, 2000; Thomas *et al.*, 2008), thus modifying DNA binding or other regulatory functions. The reversible methylation of specific glutamate residues in the cytoplasmic domains of chemoreceptors is known to control bacterial chemotaxis through a TCS signalling route (Wadhams and Armitage, 2004). Two competing enzymes control the receptor methylation status: CheR, a methyltransferase, and CheB, a methylesterase/deamidase.

In *B. cereus*, RsbY, which is homologous to RsbU and RsbP in *B. subtilis,* is required for σ[B] activation. RsbY contains a PP2C-type protein phosphatase domain in its C-terminal region, it presumably hydrolyses phosphorylated RsbV. The N-terminal domain of RsbY is homologous to the CheY-like REC domains of TCSs (van Schaik *et al.*, 2005). Based on domain analysis and genome context, de Been and co-workers proposed a model in which RsbK is a hybrid sensor kinase that controls RsbY phosphatase activity via the phosphorylation of the N-terminal REC domain of RsbY (de Been *et al.*, 2010). Therefore, σ[B] activity of *B. cereus* is likely regulated by a partner-switching mechanism associated with specific TCSs. In the present study, we reveal *bc1007* to be flanked downstream by *rsbK*, encoding a CheR-type methyltransferase that is capable of methylating RsbK and functions as a negative regulator of σ[B]. The probable methylation sites of RsbK were further assessed by residue substitution.

Results

Investigation of the role of BC1007 in σ[B] activation

The *sigB* gene cluster of *B. cereus* strain ATCC 14579 encodes an open reading frame, *bc1007*, flanking *rsbY* and *rsbK*, and the consecutive *rsbK* and *bc1007* comprise an operon (Fig. 1A). A previous study suggested that RsbK and RsbY form a TCS in which RsbK transfers a phosphoryl group to RsbY (de Been *et al.*, 2010). BC1007 is supposed to encode a methyl-accepting chemotaxis protein (MCP) methyltransferase (de Been *et al.*, 2011). However, the function of BC1007 has not yet been demonstrated. To determine whether BC1007 is involved in σ[B] regulation, the *bc1007* deletion strain KNU701 was generated in this study (Fig. 1B). The deletion of *bc1007* did not affect cell morphology or cell growth compared with the wild-type strain (data not shown). To further understand the function of *bc1007*, KNU701 was exposed to 42°C temperatures and analysed by immunoblot for the detection of the σ[B], Dps-like bacterioferritin (BC1005), and EF-TU (translation elongation factor, a housekeeping protein used as an internal control) proteins. Interestingly, in contrast to a wild-type strain, the heat stress did not influence σ[B] activity due to the high basal level in the mutant (Fig. 2A). This pattern of σ[B] expression was validated by a similar effect of the Dps-like bacterioferritin (BC1005), a member of the σ[B]-dependent regulon (Fig. 2A). In the complementary strain KNU703 harbouring pHT304-rsbK-bc1007 (Fig. 1C), σ[B] activity was similar to that observed in the wild-type control but not in the mock control strain KNU702 (Fig. 2A). This result indicated that BC1007 directly or indirectly influences σ[B] activity. As σ[B] is known to induce the transcription of genes important in the response to stress, we performed a time-course experiment to examine the effect of BC1007 on cell survival when cells were exposed to lethal temperatures. Both wild-type and KNU701 strains were subjected to heat shock with a gradually increased temperature from 30°C to 50°C, the lethal temperature, and cell viability was determined by plate count. Consistent with the σ[B] levels detected with the immunoblot (Fig. 2A), the KNU701 strain demonstrated relatively higher survival

(A)

SigmaB gene cluster

rsbV 110 aa | rsbW 160 aa | sigB 258 aa | Dps-like Bacterioferritin 148 aa | rsbY 380 aa | 1007 285 aa | rsbK 896 aa | 1009 83 aa

500 bp

(B)

pMAD 9666 pb

bla · ermCA · bgaB · pclpB · MCS · pIR232 · ori

pMAD-Δbc1007

rsbK | spc^r | rsbY
BamHI · 800 bp · MluI · 1221bp · NcoI · 1041bp · BglII

pMAD-ΔrsbK

rsbK | spc^r | rsbK | bc1007
BamHI · 739 bp · SalI · 750bp · SmaI · 1411bp · NcoI

(C)

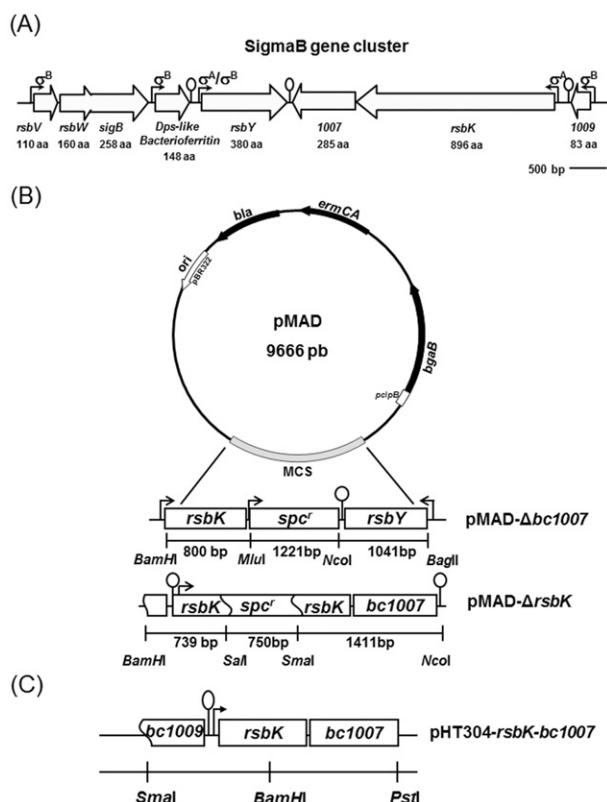bc1009 | rsbK | bc1007   pHT304-rsbK-bc1007
SmaI · BamHI · PstI

Fig. 1. Deletion of *bc1007* and *rsbK*.
A. Schematic diagram of the genetic organization of the *sigB* cluster.
B. Construction of the *bc1007* and *rsbK* knockout mutants. The *bc1007* was replaced with a spectinomycin resistance cassette with the integration vector pMAD. Similarly, the *rsbK* gene was disrupted in-frame by the insertion of the spectinomycin resistance cassette. The constructed plasmid was introduced into *Bacillus cereus* via electroporation for allelic exchange. The restriction sites and the inserted DNA length are indicated.
C. Construction of the complementary plasmid pHT304-*rsbK-bc1007*. The DNA fragment, including the partial *bc1009* and *rsbK-bc1007*, was inserted into the vector pHT304. The restriction sites are indicated.

rates when compared with the wild-type strain, particularly from 10 to 25 min (Fig. 2B).

Analysis of the interactions between RsbY, BC1007 and RsbK using the bacterial two-hybrid assay

According to the gene arrangements, our result indicated that protein–protein interactions may be occurring between the neighbouring gene products RsbY, BC1007 and RsbK. Thus, the bacterial two-hybrid system was employed to examine this potential interaction (Fig. 3A). Full-length *rsbY* and *rsbK* were first inserted into the expression vectors pKT-25 and pUT-18 respectively, and the constructs were then co-transformed into *Escherichia coli* BTH101. Colony growth on selective plates indicated a significant interaction between RsbK and RsbY

(Fig. 3B). Using a similar method, a positive phenotype on selective media also indicated a significant interaction between RsbK and BC1007, but BC1007 had no apparent interaction with RsbY (Fig. 3B). Previously, the expression of a C-terminal REC domain-truncated *rsbK* moderately increased σ^B levels in the *rsbK* deletion strain (de Been *et al.*, 2010). Therefore, we attempted to investigate whether the REC-truncated RsbK interacted with RsbY. However, the combination of RsbY and the REC-truncated RsbK did not exhibit a positive colony phenotype on MacConkey and LB selection plates (Fig. 3B), but blue colonies grown on M63 selection medium were present, indicating that the loss of the REC domain dimin-
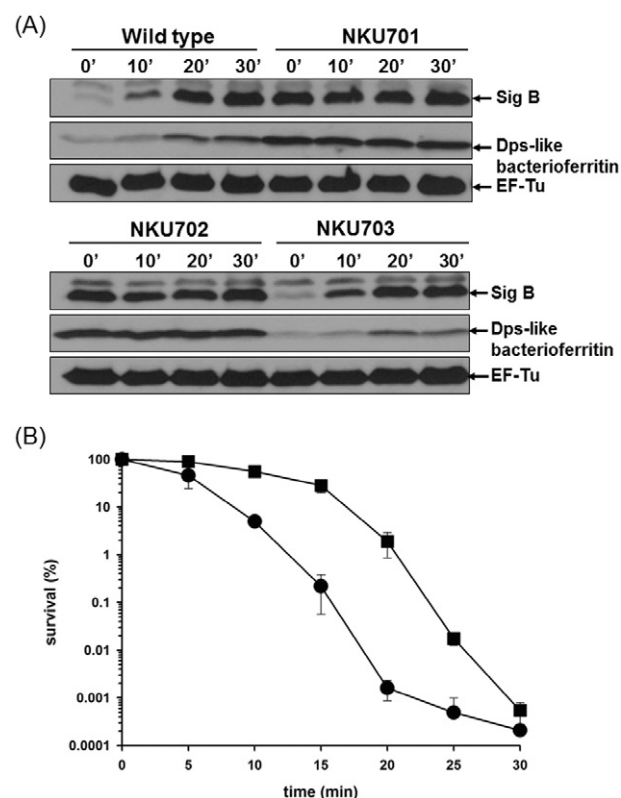
(A)

Wild type | NKU701
0' 10' 20' 30' | 0' 10' 20' 30'
← Sig B
← Dps-like bacterioferritin
← EF-Tu

NKU702 | NKU703
0' 10' 20' 30' | 0' 10' 20' 30'
← Sig B
← Dps-like bacterioferritin
← EF-Tu

(B)

survival (%) vs time (min)

Fig. 2. Effects of *bc1007* deletion on σ^B levels and heat shock protection.
A. σ^B expression as detected by immunoblotting. Cultures of *Bacillus cereus* and the *bc1007* deletion strain KNU701 were grown to the mid-exponential growth phase at 30°C and then exposed to a mild heat shock (42°C). The extracted cellular proteins at the indicated time points were subjected to Western blotting. Similarly, the KNU701 strain containing either the empty vector (pHP304) or the complementation plasmid (pHT304-*rsbK-bc1007*) was exposed to a mild heat shock (42°C), and protein expression was detected by Western blot.
B. The protective heat shock response. Cultures of *Bacillus cereus* (circles) and the derivative KNU701 strain (squares) were grown to the mid-exponential growth phase at 30°C and killed at 50°C. The averages of three independent experiments are shown. The error bars indicate standard deviations.

(A)

Plasmid pairs used for bacterial two-hybrid analysis

	Plasmid		Hybrid proteins	
1	pKT25-*zip*	pUT18-*zip*	㉕—L-L-L-L-	-L-L-L-L—⑱
2	pKT25	pUT18	㉕—C	N—⑱
3	pKT25-*rsbY*	pUT18-*rsbK* FL	㉕—[RsbY]-C	N-[RsbK]—⑱
4	pKT25-*rsbY*	pUT18-*rsbK* Trunc	㉕—[RsbY]-C	N-[RsbK]—⑱
5	pKT25-*bc1007*	pUT18-*rsbK* FL	㉕—[BC1007]-C	N-[RsbK]—⑱
6	pKT25-*rsbY*	pUT18-*bc1007*	㉕—[RsbY]-C	N-[BC1007]—⑱

■ RR receiver domain   L-L-L-L- leucine zipper of GCN4

(B)

(a) (b) (c) (d)

T+ T-

T18- rsbK trunc / T25- rsbY   T18- 1007 / T25- rsbY

T18- rsbK FL / T25- rsbY   T18- rsbK FL / T25- 1007

Fig. 3. Bacterial two-hybrid analyses of the interactions between RsbY, BC1007 and RsbK.
A. Combinations of constructed plasmids for the bacterial two-hybrid analysis. Full-length *rsbY, bc1007, rsbK* and C-terminal truncated *rsbK* were individually inserted into pUT18 or pKT25. The diagram showed various pairs of pUT18- and pKT25-derived plasmids.
B. Protein–protein interactions analysed by the bacterial two-hybrid system. *Escherichia coli* BTH101 cells containing various combinations of constructed plasmids were propagated on indicator plates. T+, pUT18-zip and pKT25-zip (positive controls); T−, pUC18 and pKT25 vectors (negative controls). (a) MacConkey/maltose; (b) LB/X-Gal; (c) M63/maltose X-Gal; (d) Different gene combinations are denoted.
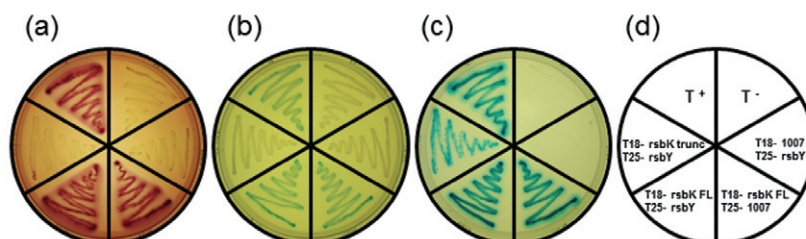
ished the protein interaction between RsbK and RsbY. Our data reveal that RsbK interacts directly not only with RsbY but also with BC1007.

Methylation of RsbK by BC1007 *in vitro*

The results of the two-hybrid analysis indicated that RsbK interacts with BC1007, but the nature of the interaction remains unknown. We cloned both the intact *rsbK* gene and *rsbK-bc1007* individually into the expression vector pET21b to overexpress His-tagged RsbK (RsbK-His$_6$) or His$_6$-tagged BC1007 (BC1007-His$_6$) to determine whether RsbK is the target protein for BC1007. The protein levels of purified BC1007 and overexpressed His-tagged RsbK of *E. coli* cell lysate were resolved by SDS-PAGE, in which RsbK-His$_6$ (Fig. 4A, lanes 2 and 3) and two other protein bands representing BC1007-His$_6$ and its degraded derivative BC1007-His$_6$ (Fig. 4A, lanes 1 and 3) were visualized. The presence of each protein was confirmed by Western blot using anti-His$_6$ monoclonal antibody, and RsbK-His$_6$ was further verified by mass spectrometry (data not shown). To conduct RsbK methylation *in vitro*, cell lysates derived from His-tagged RsbK overexpression in *E. coli* (Fig. 4A) were incubated with the purified

BC1007-His$_6$ in the presence of C^{14}-methyl-labelled S-adenosylmethionine (SAM) and subjected to autoradiography. As a control, C^{14}-methyl SAM was also incubated individually with the His-tagged RsbK cell lysate (Fig. 4B, lane 2) and the purified BC1007-His$_6$ (Fig. 4B, lane 1). A radiolabelled signal clearly appeared at the molecular weight corresponding to RsbK when the purified BC1007-His$_6$ was mixed with the His-tagged RsbK cell lysate (Fig. 4B, lane 3). This signal could not be attributed to endogenous *E. coli* methyltransferases because no signal was observed in the control reactions (Fig. 4B, lane 2). The result demonstrated that BC1007 is able to specifically transfer the methyl group(s) from SAM to RsbK.

Identification of putative methylation sites by site-directed mutagenesis

Although our data demonstrated that RsbK can be methylated by BC1007 *in vitro*, it is still unclear which residue(s) in RsbK is/are methylated. Recently, a systematic analysis suggested that potential methylation substrates have conserved glutamate and glutamine residues at the 'b' and 'c' positions of the 'a-b-c-d-e-f-g' coiled-coil heptad repeat
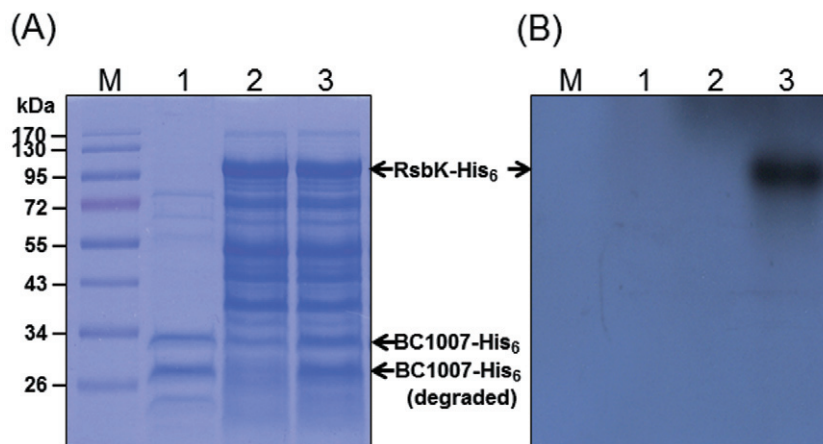
Fig. 4. Methylation of RsbK by purified BC1007 *in vitro*.
A. The overexpressed His-tagged RsbK of the *Escherichia coli* cell lysate and purified His-tagged BC1007 were used in the methylation assay. Proteins were resolved on 12% SDS-PAGE followed by Coomassie blue staining. RsbK-His$_6$ and BC1007-His$_6$ are indicated by arrows; purified BC1007-His$_6$ isolated from *E. coli* BL21 (λDE3) overexpressed with pET21b-*rsbK-bc1007* (lane 1); 100 μg of cell lysate derived from His-tagged RsbK overexpression in *E. coli* (lane 2); a mixture of purified BC1007 and cell lysates derived from His-tagged RsbK overexpression in *E. coli* (lane 3).
B. *In vitro* methylation. The methylation reaction was conducted by the addition of [^{14}C]SAM into purified BC1007 (lane 1), cell lysates derived from His-tagged RsbK overexpression in *E. coli* (lane 2) or the mixture of purified BC1007 and cell lysates derived from His-tagged RsbK overexpression in *E. coli* (lane 3), and the gel was subjected to autoradiography. Radiolabelled RsbK is indicated by an arrow.

(Terwilliger *et al.*, 1986; Nowlin *et al.*, 1987; Le Moual and Koshland, 1996; Perez *et al.*, 2006). The presence of six methylation consensus sequences from Glu^{431} to Thr^{472} in RsbK has been proposed, indicating 12 putative methylation sites at conserved glutamate and glutamine residues (Fig. 5A) (de Been *et al.*, 2011). We studied the function of these putative RsbK methylation sites by constructing 24 RsbK methylation point mutants (*rsbK$_m$*) (Table S2) where a methylatable glutamate residue was replaced with either an aspartate or an alanine residue. These substitutions were used in other bacteria to mimic unmethylated and methylated glutamates respectively. The aspartate residues, which cannot be methylated, maintain the negative charge of a glutamate residue, whereas the naturally charged alanine residues, similar to methyl esterified glutamates, cause less perturbation to the predicted α-helix (Nowlin *et al.*, 1988; Park *et al.*, 1990; Shapiro and Koshland, 1994).

The intact operon *rsbK$_m$-bc1007* was then cloned into the low-copy vector pHT304, and the resulting plasmid pHT304-*rsbK$_m$-bc1007* was introduced into the *rsbK* deletion strain (KNU802). Subsequently, σ^B levels were analysed by Western blot in each strain after 42°C exposure. σ^B activation was abolished in KNU802 compared with the wild-type strain (Fig. 5B). However, σ^B activation was restored when KNU802 was complemented with the pHT304-*rsbK-bc1007* plasmid. Similarly, restoration of σ^B activity was observed when KNU802 harboured any of the plasmids expressing various RsbK methylation mutations, except for RsbK$_{E439A}$, and lower expression levels of σ^B

were observed when complemented with RsbK$_{E446A}$ (Fig. 5B). These data indicated that Glu^{439} might be a preferential methylation site and Glu^{446} a potential secondary site for methylation. Our data demonstrated that alanyl substitution on Glu^{439} or Glu^{446} significantly impaired σ^B induction in the KNU802 strain. Therefore, we expected that aspartyl substitution, mimicking demethylation of these residues, would result in relatively high levels of σ^B even in the absence of stress. However, only basal levels of σ^B were detected prior to 42°C exposure, and the σ^B induction profile under heat stress was comparable to that of the wild-type. These results imply that the lack of methylation at any of these residues is insufficient to cause σ^B activation.

Discussion

Multiple studies have demonstrated the roles of *rsbV, rsbW, sigB, rsbY* and *rsbK* in σ^B regulation in *B. cereus* (van Schaik *et al.*, 2004; van Schaik *et al.*, 2005; de Been *et al.*, 2010). In addition to these regulatory proteins, the *sigB* gene cluster also encodes a *dps-like bacterioferritin* (*bc1005*), dispensable for σ^B activity (Wang *et al.*, 2009), as well as *bc1007* (Fig. 1A). In the present study, we performed a genetic deletion study of *bc1007* using recombinant DNA methods and revealed that *bc1007* deletion constitutively induced high levels of σ^B irrespective of heat stress, leading to increased viability relative to the wild-type strain upon lethal heat exposure (Figs 1B and 2A). These results signify the participation of BC1007
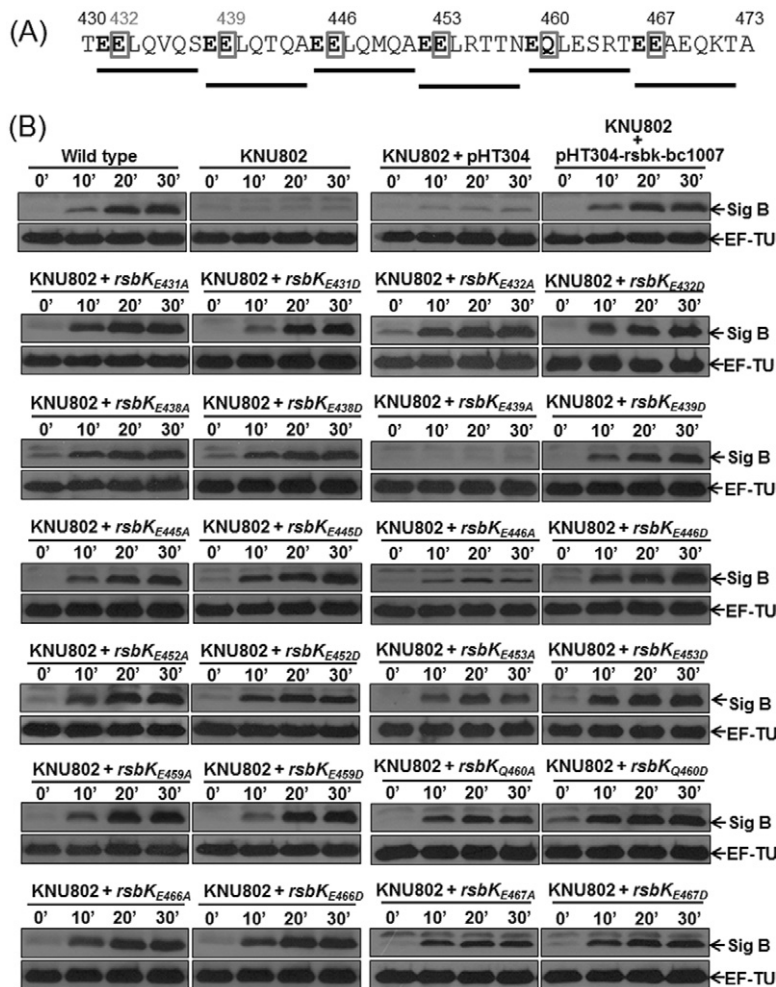
Fig. 5. Effects of RsbK mutants on σ^B activity.
A. Predicted methylation sites in RsbK. The heptad repeat regions of methylation consensus sequences are underlined. Predicted methylation sites are indicated by bold letters, and the box denotes the second residue of the methylation pair. Numbers depict amino acid positions in RsbK.
B. The influence of RsbK mutant expression on σ^B activation. The plasmid pTH304-*rsbKm-bc1007* was constructed, and *rsbK$_m$* represents the residue substitution on the predicted methylation site in RsbK: glutamate/glutamine with alanine mimics methylation, and glutamate/glutamine with aspartate mimics demethylation. The constructed plasmids were transformed separately into the *Bacillus cereus* strain KNU802, and the resulting strains were heated to 42°C for the indicated time periods. Cellular extracts were subjected to Western blot analysis.

in σ^B regulation, but it may be argued that the high level of σ^B expression could be caused either by *bc1007* deletion or due to an unexpected polarity. However, the high constitutive σ^B activity was restored in KNU703 after the introduction of the complementary plasmid pHT304-*rsbK-bc1007* (Figs 1C and 2A), and any interference of the *rsbY* or *rsbK* genes flanking *bc1007* should inactivate σ^B (van Schaik *et al*., 2005; de Been *et al*., 2010). Thus, the high constitutive expression of σ^B is simply a consequence of the *bc1007* knockout.

We were interested in understanding how BC1007 regulates σ^B activity. The *bc1007* and *rsbK* genes have been shown to be transcribed by a σ^A-dependent promoter immediately upstream of *rsbK*, generating a polycistronic mRNA (Fig. 1A). The architectural complexity of the functional domains indicate that RsbK acts as a multiple hybrid sensor kinase, presumably regulating RsbY through a TCS signalling pathway in response to external and internal changes (de Been *et al*., 2011). BC1007 has been proposed to display MCP methyltransferase activity (de Been *et al*., 2011). In the original genome sequence of

B. cereus ATCC 14579 (Ivanova *et al*., 2003), the product of *bc1007* was annotated as a chemotaxis protein methyltransferase (http://www.ncbi.nlm.nih.gov/gene/1203356) with 28% and 29% identity with *E. coli* CheR (GI:145523) and *B. subtilis* CheR (GI:143805) respectively. BC1007 contains a conserved N-terminal all alpha domain from Asn[19] to Gly[73] and a C-terminal SAM binding domain from Asn[85] to Arg[263], based on the protein domain information extracted from Pfam (Punta *et al*., 2012, http://pfam.sanger.ac.uk/protein/Q81H19). Therefore, BC1007 potentially regulates σ^B through direct interaction with RsbK. This assumption is supported by two lines of evidence: (i) the bacterial two-hybrid analysis showed that BC1007 only interacted with RsbK and not with RsbY (Fig. 3) or other regulators in the *sigB* cluster (data not shown), and (ii) autoradiography showed that the C[14]-methyl group(s) was specifically transferred from radiolabelled SAM to RsbK when RsbK was incubated with BC1007 (Fig. 4). Collectively, we conclude that BC1007 is the cognate methyltransferase of RsbK and functions as a negative regulator of σ^B.

We employed site-directed mutagenesis to determine which residue(s) out of 12 putative methylation sites was potentially methyl-modified under environmental stress. As shown in Fig. 5B, most of the RsbK mutants were capable of inducing σ^B expression (similar to the wild-type RsbK), but with RsbK$_{E439A}$, σ^B levels remained low, suggesting that the Glu^{439} residue might be the preferential methylation site critical for σ^B control *in vivo*. In contrast, alanyl substitution on Glu^{446} resulted in only minimal σ^B repression. This attenuated σ^B activation due to RsbK$_{E446A}$ could be explained by two hypotheses. First, the residue substitution is not exactly the same mechanistically as a methylated glutamyl residue, although alanyl replacement eliminates the negative charge of Glu^{446}. Second, the residue change on Glu^{446} may neutralize the negative charge, creating a structural constraint and thereby interfering with proper σ^B inhibition due to the close proximity of the Glu^{439} methylation site. This explanation is plausible because methylation sites have been reported to be spaced evenly at seven-residue intervals on the same face of the α-helix where they are accessible to the methyltransferase (Terwilliger *et al.*, 1986). Alanyl substitutions on Glu^{439} and Glu^{446} inhibited σ^B to different extents, but the expression of RsbK$_{E439D}$ and RsbK$_{E446D}$, which remain the predicted methylatable Glu^{446} and Glu^{439} respectively, rescued σ^B induction, similar to that observed in the wild-type strain (Fig. 5B). These results suggest that methylation of any of the methylatable sites may be sufficient to repress σ^B, whereas methylation of one or more residues in RsbK may occur *in vivo*. This pattern may reflect a subtle methylation pattern in RsbK that fine tunes the level of σ^B induction in response to various stimulation strengths or distinct environmental stressors. In accordance with this postulation, a previous study has shown *B. cereus* treated with 2.5% NaCl to demonstrate a weak level of σ^B activation compared with the bacteria receiving the 42°C heat stress treatment (de Been *et al.*, 2010). Although site-directed mutagenesis was employed at the speculated methylatable positions in this study, substantial techniques such as mass spectrometry need to be used to reflect the *in vivo* methylation of wild-type RsbK under physiological conditions because mutagenization not only eliminates the putative methylatable residue but also modifies the BC1007 recognition sequence.

Methylation of MCPs in bacterial TCSs is often associated with sensory adaptation to diverse environmental stimuli (Kirby, 2009). In *E. coli*, chemotaxis is mediated by methylation, producing the increased kinase activity of the MCP-associated CheA (Surette and Stock, 1996; Glekas *et al.*, 2011). Modulation of CheA activity through the methylation of MCPs at given sites differentially regulates chemotaxis in *B. subtilis* (Glekas *et al.*, 2011) and cellular development in *Myxococcus xanthus* (Scott

et al., 2008). Similar protein interactions have been mechanistically linked to diverse cellular functions, including intracellular levels of cyclic di-GMP, growth, biofilm formation and cell development via functionally and spatially distinct signalling pathways (D'Argenio *et al.*, 2002; Kirby and Zusman, 2003; Berleman and Bauer, 2005; Tran *et al.*, 2008). We demonstrate here for the first time the successful activation of an alternative transcription factor to be governed by BC1007, a CheR-type methylatransferase. Although *bc1007* encodes a CheR-type methylatransferase, *bc1007* is not relevant to chemotaxis because deletion of *bc1007* did not impair the bacteria's motility compared with the wild-type strain (data not shown). Notably, multiple homologues of associated methyltransferases (CheR) and methylesterases (CheB) are found in other bacteria (Falke *et al.*, 1997; Martin *et al.*, 2001; Kanungpean *et al.*, 2011), but full genome searches revealed no CheB homologues that could be responsible for demethylation in *B. cereus*. The mechanism of the relief of BC1007-mediated inhibition remains unknown. Homodimers are known to be functional units in a few chemoreceptors and histidine kinases, and the HAMP domain signalling mechanisms are likely intimately tied to this structural organization (Parkinson, 2010). It would be interesting to know whether RsbK forms a functional dimer as RsbK contains a cytoplasmic HAMP domain. If so, is it possible that the methyl group(s) of RsbK constitute(s) steric hindrances destabilizing RsbK dimerization? In addition, in the BC1007 deletion mutant, all RsbK methylation sites are expected to be demethylated. As shown in Fig. 2A, this demethylation leads to constitutive σ^B activation even when there is no stress. Therefore, one may assume that under non-stress conditions, a certain degree of RsbK methylation keeps σ^B levels in check.

A previous study using genetic approaches suggested that RsbK activates RsbY via either direct phosphoryl transfer from the HK domain of RsbK to the REC domain of RsbY or a multi-step phosphotransfer route in which RsbK first transfers phosphoryl from its HK domain to its own REC domain, after which phosphoryl is transferred to the RsbY REC domain via a third phosphotransferase protein (de Been *et al.*, 2010). Our bacterial two-hybrid results demonstrated a strong interaction between full-length RsbK and RsbY (Fig. 1B and C), indicating that the σ^B signalling pathway can be mediated by direct phosphotransfer. Additionally, the RR-truncated RsbK retained a weak interaction with RsbY, which may explain why the expression of the RR-truncated RsbK elevated σ^B expression in the *rsbK* deletion strain but never reached the maximum level (de Been *et al.*, 2010). Our results indicated that the REC domain is required for maintaining RsbK in a proper conformation that allows RsbK interaction with RsbY. Previously, the phosphorylation state

(D827) of the REC domain in RsbK has been proposed to modulate the efficiency of phosphorelay (de Been *et al.*, 2010). Similar regulatory mechanisms have been shown in other organisms, such as ArcB in *E. coli* (Iuchi, 1993) and VsrB in *Pseudomonas solanacearum* (Huang *et al.*, 1993). A recent study suggested that the phosphorylation of the C-terminal RR domains of VirA functions as an activator to increase phosphotransfer from VirA to VirG in *Agrobacterium tumefaciens* (Wise *et al.*, 2010). The role of the phosphorylation of D827 in the REC domain requires further investigation.

Gene arrays of the *rsbK* orthologues and the neighbouring *rsbY* and *bc1007* orthologues were not restricted to members of the *B. cereus* group but found in a wide range of bacteria, suggesting that the RsbK-M-Y signalling is a common regulatory strategy in bacteria (de Been *et al.*, 2011). In this study, two heptad segments enclose RsbK potential methylation residue Glu^{439} and Glu^{446} may play critical roles for σ^B control. We use sequence logo (Crooks *et al.*, 2004; http://weblogo.threeplusone.com/) to describe the conserved pattern of these two heptads. Homologue sequences were constructed from the members in KEGG (Kyoto Encyclopedia of Genes and Genomes) SSDB (Sequence Similarity DataBase) (Kanehisa *et al.*, 2012) RsbK gene clusters, which are summarized according to the orthologous relationship by both sequence similarity and genome organization among 1490 Bacterial genomes, 118 Archaeal genomes, and 171 Eukaryotic genomes (in March 2012). In the highly conserved orthologue gene cluster set, 127 RsbK-like sequences are found in 10 bacteria phyla (Table S3) to have BC1007 homologues as a close neighbour and these two genes are arranged in the same orientation. No orthologue was found in Archaea and Eukaryotes. Although some sequences from *Cyanobacteria, Deinococcus-Thermus* and *Deltaproteobacteria* show poor alignment, all of these sequences retain the perfect leucine residue repeat (one leucine per seven residues) (Fig. S1A). As shown in the sequence logo (Fig. S1B), residue composition of the 'c' position of potential methylation site (e.g. Glu^{439}) is highly conserved, and the overall composition of first heptad (Glu^{439} enclosed heptad) is more conserved than the second heptad containing Glu^{446}.

In summary, our results indicate that the methylation of RsbK by a CheR-like methyltransferase BC1007 (renamed RsbM: Regulator of sigmaB Methyltransferase) could inhibit σ^B activation in the absence of stress. When a stress signal occurs, the activated RsbK propagates the signal to downstream regulators (RsbY, RsbV, RsbW) to release and activate σ^B (Fig. 6). This finding expands our understanding of the common RsbK-M-Y module that controls a diverse array of signalling networks, particularly those containing σ^B-like stress factors.
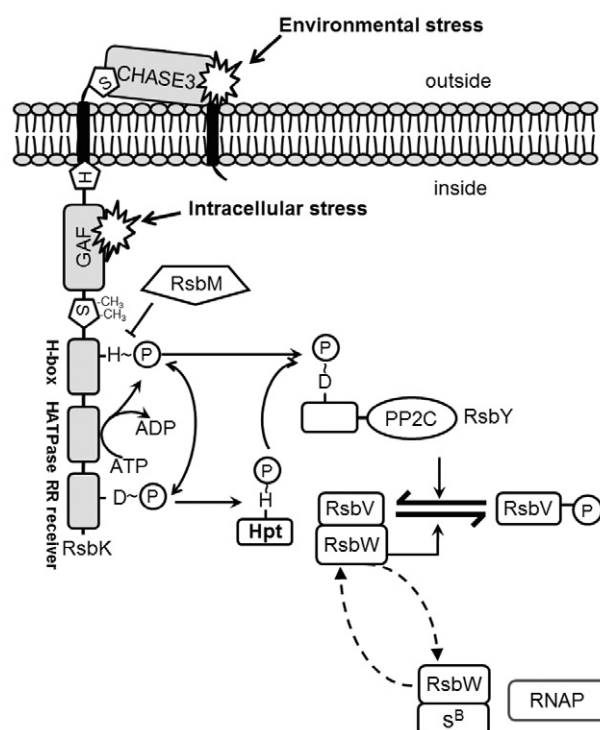

Fig. 6. Models for σ^B activation in *Bacillus cereus*. In the absence of stress, σ^B is maintained inactive in a complex with its anti-sigma factor RsbW, which also inactivates RsbV by phosphorylation through its kinase activity. RsbM (BC1007) methylates RsbK on residues Glu^{439} and Glu^{446} and thereby inhibits σ^B activity. If stimulated by specific stress signals, RsbK is activated, and the phosphate directly transferred from the H-box of RsbK to the REC domain of RsbY or indirectly transferred through a multi-step phosphotransfer route in which RsbK first transfers phosphoryl from its HK domain to its own REC domain, after which phosphoryl is transferred to the REC domain of RsbY via a third histidine-containing phosphotransferase (Hpt) protein (de Been *et al.*, 2010). This action enhances the phosphatase activity of RsbY to hydrolyse RsbV-P. The RsbW : σ^B complex is disrupted the dephosphorylated RsbV because RsbW forms an alternative complex with RsbV (dashed arrows). Free σ^B can now interact with RNA polymerase and induce direct transcription of the SigB-dependent general stress response genes.

Experimental procedures

Bacterial strains and plasmids

The genotypes and sources of the bacterial strains and plasmids used in this study are listed in Table S1. *Bacillus cereus* (ATCC 14579) was grown in brain heart infusion (BHI) medium at 30°C, and *E. coli* was cultured in Luria-Bertani (LB) medium at 37°C. The *E. coli* strains DH5-α, XL-1 blue and BL21 (λDE3) were used for plasmid manipulation and IPTG-induced expression. The growth of the cultures was monitored by measuring the optical density at 600 nm (OD$_{600}$). The antibiotic selection used for cloning and mutant screening was performed with ampicillin (50 μg ml^{-1}), erythromycin (3 μg ml^{-1}), and spectinomycin (100 μg ml^{-1}), as required.

Bacterial two-hybrid assay

Bacterial two-hybrid analysis of protein interactions was performed as previously described (Karimova *et al.*, 1998). To construct recombinant plasmids for use in bacterial two-hybrid analysis, *rsbY, bc1007, rsbK* and C-terminal truncated *rsbK* were amplified by PCR using specific oligonucleotide primers (Table S2). The amplicons, *bc1007, rsbK* and C-terminal truncated *rsbK,* were individually cloned in-frame into the multiple cloning site of pUT18. The amplicons*, rsbY* and *bc1007,* were cloned into pKT25 individually. Complementation of protein pairs (Fig. 3) was indicated by blue colony growth on LB plates containing X-gal, by blue colony growth on M63-defined medium/maltose containing 0.5 mM IPTG and 40 µg ml⁻¹ X-gal or by red colony growth on MacConkey-maltose agar. Both media contained ampicillin and kanamycin to select for the inserted plasmids. The plates were incubated at 30°C for a maximum of 40 h. The pKT25-zip and pUT18-zip plasmids were used as positive controls for protein interaction, and the empty vectors pKT25 and pUT18 were used as negative controls.

Construction of bc1007 *and* rsbK *null strains*

Gene deletion of *bc1007* and *rsbK* was performed as previously described (Arnaud *et al.*, 2004). To produce the pMAD-Δbc1007 plasmid, two DNA fragments of 800 bp and 1041 bp, corresponding to the regions located directly upstream and downstream of *bc1007* respectively, were amplified by PCR using *B. cereus* genomic DNA as the template. Using restriction enzymes, these DNA fragments were cloned into the pMAD vector on either side of a DNA fragment (1221 bp) that was amplified by PCR from pDG1728. Similarly, a 739 bp DNA fragment, beginning 424 bp upstream of *rsbK* and continuing through 315 bp of the 5′ coding region, and an additional 1411 bp DNA fragment, beginning at 447 bp of the 3′ end and ending 964 bp downstream of *rsbK,* were amplified from *B. cereus* genomic DNA. To generate pMAD-Δ*rsbK*, the coding region of the spectinomycin resistance gene (750 bp) was inserted in-frame into the above DNA fragments. Oligonucleotide primers used are shown in Table S2, and the plasmid map is indicated in Fig. 1B. Both the pMAD-Δ*bc1007* and pMAD-Δ*rsbK* plasmids were introduced into *B. cereus* by electroporation at 1.7 kV in 1 cm electrocuvettes (Eppendorf). Transformants were obtained after culturing for 2 days at 30°C on BHI plates containing spectinomycin, erythromycin, and X-gal. A pool of individual transformants was used to inoculate a culture of BHI medium without antibiotics, and this culture was then incubated at 40°C until the stationary phase of growth was reached. Two additional growth cycles were performed by diluting the stationary phase culture into fresh media, and single colonies were isolated by plating dilutions of the culture overnight onto BHI plates containing X-gal and spectinomycin. Several white colonies were also isolated to verify the erythromycin-sensitive phenotype. DNA was purified from several clones and analysed by PCR using oligonucleotides that hybridized outside of the inserts to verify the presence of the deletion and the insertion of the spectinomycin resistance gene. Gene deletion was also confirmed by Southern blot. The *bc1007* and *rsbK* deletion mutant strains were named KNU701 and KNU802 respectively.

Construction of pHT304-rsbK-bc1007 *and pHT304*-rsbKₘ-bc1007

A DNA fragment (2255 bp) containing a partial sequence from *bc1009* and internal to *rsbK* with the endogenous BamHI site was amplified by PCR from the genomic DNA of *B. cereus* using the Restore-up-SmaI-F and Restore-up-BamHI-R primers (Table S2). Another DNA fragment (1782 bp), which included the rest of *rsbK* and full-length *bc1007,* was amplified with the Restore-do-BamHI-F and Restore-do-PstI-R primers (Table S2). Both DNA fragments were then inserted into pHT304 to generate pHT304-*rsbK-bc1007* (Fig. 1C). Complementation of the *bc1007* mutation found in strain KNU701 was performed by introduction into the plasmid pHT304-*rsbK-bc1007,* thus generating strain KNU703. The plasmid control (mock) strain KNU702 was generated by introducing the pHT304 plasmid into the KNU701 strain.

Site-directed mutagenesis was performed as previously described (Ho *et al.*, 1989; Kanoksilapatham *et al.*, 2007), with slight modifications to generate the vector carrying the mutagenic *rsbK*, pHT304-*rsbKₘ-bc1007*. A standard PCR reaction (50 µl) was conducted in Phusion™ GC buffer containing pHT304-*rsbK-bc1007* (30 ng) as the template and 1 U Phusion™ high-fidelity DNA polymerase (NEB) in 3% DMSO using the primer pairs listed in Table S2. The PCR product was digested with the DpnI restriction enzyme to cleave the methylated pHT304-*rsbK-bc1007* template and then transformed into the *E. coli* XL-1 blue strain. The mutagenized plasmid was extracted, and the mutations were confirmed by DNA sequencing.

Construction of pET21b-rsbK *and pET21b*-rsbK-bc1007-*6xHis*

The entire *rsbK* coding region was PCR amplified from the genomic DNA of *B. cereus* using the primers pET21b-rsbK-NdeI-F and pET21b-rsbK-XhoI-R. The PCR product was digested by NdeI and XhoI and cloned into the plasmid pET21b to generate the plasmid pET21b-*rsbK* (Table S1). In addition, the full-length reading frame of the *rsbK-bc1007* operon with the deletion of the stop codon was cloned into the expression vector pET21b to construct pET21b-*rsbK-bc1007-6xHis* (Table S1). For this purpose, the DNA fragment from the first codon of *rsbK* to the region containing the only intrinsic BamHI restriction site of *rsbK* and another DNA fragment from the intrinsic BamHI restriction site to the terminator of *bc1007,* were amplified with primer pairs with restriction sites introduced (Table S2). Subsequently, the two PCR products were digested with NdeI/BamHI and BamHI/XhoI respectively, and inserted into pET21b.

Western blot

Bacillus cereus and the engineered derivatives were grown in BHI broth at 30°C with aeration until an OD₆₀₀ of 0.5 was reached. They were then incubated at 42°C for 10, 20 and 30 min. The cells were pelleted by centrifugation and immediately frozen in liquid nitrogen. The cells were subsequently disrupted by sonication. Cell extracts (30 µg) were separated

by SDS-PAGE and transferred onto nitrocellulose membranes. The membranes were probed with 1:5000 dilutions of anti-σ^B, anti-Dps-like bacterioferritin (BC1005), and anti-EF-TU (BC0129) polyclonal antisera in PBS-Tween at room temperature for 1 h with gentle agitation. The membranes were then incubated with a secondary antibody (HRP-conjugated goat anti-rabbit IgG). For the detection of His-tagged RsbK expression in *E. coli*, the membranes were blotted with a 1:2000 dilution of an anti-His tag monoclonal antibody followed by incubation with a secondary antibody (HRP-conjugated goat anti-mouse IgG). Enhanced chemiluminescence detection reagents were added to develop the images.

Cell viability experiments

Wild-type *B. cereus* and KNU701 strains were cultured until an OD_{600} of 0.5 was reached, and the cells were exposed to a lethal temperature of 50°C by shifting the whole cell culture flask from a 30°C to a 50°C water bath, causing a gradual increase in the temperature. Samples from each bacterial culture (100 μl) were taken at the indicated time points (0, 5, 10, 15, 20, 25 and 30 min), streaked onto BHI agar plates at the appropriate dilutions and incubated overnight at 30°C. Cell survival was assessed by counting the colony number and cell viability for each time point. The results were calculated from at least three independent experiments.

Protein overexpression and purification

For the purification of BC1007, *E. coli* BL21 (λDE3) cells were transformed with pET21b-*rsbK-bc1007*. Transformed cells were inoculated in 250 ml of LB medium containing 50 mg ml^{-1} ampicillin and grown at 37°C with vigorous shaking. At an OD_{600} of 0.6, protein expression was induced for 3 h by adding IPTG (isopropyl-β-D-thiogalactopyranoside) to a final concentration of 0.5 mM. Subsequently, the culture was chilled over ice, and the cells were harvested. The recombinant His$_6$-fused BC1007 protein was then purified. Briefly, harvested cells were suspended in 30 ml of cell lysis buffer [50 mM Tris–HCl (pH 8.5), 10 mM EDTA, 5 mM DTT and 1 mM phenylmethanesulfonylfluoride] and sonicated. Soluble proteins were separated from the cell debris by centrifugation at 15 000 *g* for 30 min at 4°C, and the supernatant was passed through a 0.22 μm filter (Millipore) and loaded onto a nickel column (GE Healthcare). Bound proteins were eluted according to the manufacturer's instruction.

In vitro *methylation assay*

For the overproduction of RsbK, *E. coli* BL21 (λDE3) cells were transformed with pET21b-rsbK. As described previously, the cells were harvested by centrifugation at 6000 *g* for 10 min at 4°C after IPTG induction, washed with cold PBS and then re-suspended with methylation buffer [50 mM Hepes (pH 8.0), 0.01% (v/v) NP-40, 10 mM NaCl, 1 mM DTT, 1 mM PMSF]. The collected cells were disrupted by sonication to prepare whole cell lysates, and 100 μg of each cell lysate was incubated with purified recombinant BC1007 protein in 45 μl of methylation buffer supplemented with

500 nCi of S-adenosyl-L-(methyl-^{14}C) methionine (^{14}C-SAM; 61 mCi mmol^{-1}, GE Healthcare) (radioactive methylation) for 1 h at room temperature. The reactions were stopped by adding $3 \times 10\%$ SDS-PAGE sample buffer [187.5 mM Tris-HCl, 6% (w/v) SDS, 10% glycerol, 0.03% (w/v) bromophenol blue, 1.25 M DTT, pH 6.8] followed by heating at 95°C for 10 min. The samples were analysed by 12% SDS-PAGE and stained with Coomassie blue. The gel was treated with Amplify Fluorographic Reagent (GE Healthcare) for 30 min, according to the manufacturer's instruction, and dried by vacuum. The radioactivity was visualized by exposing the gel to an X-ray film at −80°C for 1 week.

Analysis of conservation of putative methylation sites in RsbK-like proteins

To further describe the conserved pattern of the putative RsbK methylation sites, we collect *B. cererus* RsbK orthologue from KEGG SSDB (Kanehisa *et al.*, 2012) for concluding the consensus signature. In order to avoid the bias of concluding methylation site consensus pattern from an over-representative species with multiple RsbK sequences in the dataset, one sequence was picked for a single species regardless of strain diversity. Totally 79 sequences from *Proteobacteria* (48 seqs), *Firmicutes* (15 seqs), *Actinobacteria* (two seqs), *Spirochaetes* (two seqs), *Bacteroidetes* (nine seqs), *Cyanobacteria* (one seq) and Deinococcus-Thermus (two seqs), were used in this study (Table S3). Peptide sequence segments corresponding to the T421-K495 were identified by multiple sequence alignment (msa) using by Parallel PRRN in GenomeNet (Gotoh, 1995) and extended to include 10 more residues in N′ end. The final msa for the methylation sites are performed by ClustalW (Larkin *et al.*, 2007) with 'slow/accurate algorithm' and 'iterate each alignment steps'. The sequence logo of potential methylation sites of RsbK family members are constructed from msa alignment by WebLogo 3.2 (Crooks *et al.*, 2004, http://weblogo.threeplusone.com/) with a colour scheme to show the chemistry property of residues. Both the signature of *Firmicutes* sequences and of all 10 phyla sequences were concluded.

References

Agata, N., Ohta, M., and Mori, M. (1996) Production of an emetic toxin, cereulide, is associated with a specific class of *Bacillus cereus*. *Curr Microbiol* **33:** 67–69.

Alper, S., Dufour, A., Garsin, D.A., Duncan, L., and Losick, R. (1996) Role of adenosine nucleotides in the regulation of a stress-response transcription factor in *Bacillus subtilis*. *J Mol Biol* **260:** 165–177.

Arnaud, M., Chastanet, A., and Debarbouille, M. (2004) New vector for efficient allelic replacement in naturally nontransformable, low-GC-content, gram-positive bacteria. *Appl Environ Microbiol* **70:** 6887–6891.

de Been, M., Tempelaars, M.H., van Schaik, W., Moezelaar, R., Siezen, R.J., and Abee, T. (2010) A novel hybrid kinase is essential for regulating the σB-mediated stress response of *Bacillus cereus. Environ Microbiol* **12:** 730–745.

de Been, M., Francke, C., Siezen, R.J., and Abee, T. (2011) Novel σB regulation modules of Gram-positive bacteria involve the use of complex hybrid histidine kinases. *Microbiology* **157:** 3–12.

Berleman, J.E., and Bauer, C.E. (2005) Involvement of a Che-like signal transduction cascade in regulating cyst cell development in *Rhodospirillum centenum. Mol Microbiol* **56:** 1457–1466.

Bijlsma, J.J.E., and Groisman, E.A. (2003) Making informed decisions: regulatory interactions between two-component systems. *Trends Microbiol* **11:** 359–366.

Crooks, G.E., Hon, G., Chandonia, J.-M., and Brenner, S.E. (2004) WebLogo: a sequence logo generator. *Genome Res* **14:** 1188–1190.

D'Argenio, D.A., Calfee, M.W., Rainey, P.B., and Pesci, E.C. (2002) Autolysis and autoaggregation in *Pseudomonas aeruginosa* colony morphology mutants. *J Bacteriol* **184:** 6481–6289.

Delumeau, O., Lewis, R.J., and Yudkin, M.D. (2002) Protein-protein interactions that regulate the energy stress activation of σ^B in *Bacillus subtilis. J Bacteriol* **184:** 5583–5589.

Ehling-Schulz, M., Fricker, M., and Scherer, S. (2004) *Bacillus cereus*, the causative agent of an emetic type of foodborne illness. *Mol Nutr Food Res* **48:** 479–487.

Falke, J.J., Bass, R.B., Butler, S.L., Chervitz, S.A., and Danielson, M.A. (1997) The two-component signaling pathway of bacterial chemotaxis: a molecular view of signal transduction by receptors, kinases, and adaptation enzymes. *Annu Rev Cell Dev Biol* **13:** 457–512.

Galperin, M.Y. (2006) Structural classification of bacterial response regulators: diversity of output domains and domain combinations. *J Bacteriol* **188:** 4169–4182.

Glekas, G.D., Cates, J.R., Cohen, T.M., Rao, C.V., and Ordal, G.W. (2011) Site-specific methylation in *Bacillus subtilis* chemotaxis: effect of covalent modifications to the chemotaxis receptor McpB. *Microbiology* **157:** 56–65.

Gotoh, O. (1995) A weighting system and algorithm for aligning many phylogenetically related sequences. *Comput Appl Biosci* **11:** 543–551.

Gruber, T.M., and Gross, C.A. (2003) Multiple sigma subunits and the partitioning of bacterial transcription space. *Annu Rev Microbiol* **57:** 441–466.

Hecker, M., Pané-Farré, J., and Völker, U. (2007) SigB-dependent general stress response in *Bacillus subtilis* and related gram-positive bacteria. *Annu Rev Microbiol* **61:** 215–236.

Ho, S.N., Hunt, H.D., Horton, R.M., Pullen, J.K., and Pease, L.R. (1989) Site-directed mutagenesis by overlap extension using the polymerase chain reaction. *Gene* **77:** 51–59.

Hoch, A.L., and Silhavy, T.J. (1995) *Two-Component Signal Transduction*. Washington, DC, USA: American Society for Microbiology Press.

Hoch, J.A. (2000) Two-component and phosphorelay signal transduction. *Curr Opin Microbiol* **3:** 165–170.

Huang, J., Denny, T.P., and Schell, M.A. (1993) vsrB, a regulator of virulence genes of *Pseudomonas solanacearum*, is homologous to sensors of the two-component regulator family. *J Bacteriol* **175:** 6169–6178.

Iuchi, S. (1993) Phosphorylation/dephosphorylation of the receiver module at the conserved aspartate residue controls transphosphorylation activity of histidine kinase in sensor protein ArcB of *Escherichia coli. J Biol Chem* **268:** 23972–23980.

Ivanova, N., Sorokin, A., Anderson, I., Galleron, N., Candelon, B., Kapatral, V., *et al.* (2003) Genome sequence of *Bacillus cereus* and comparative analysis with *Bacillus anthracis. Nature* **423:** 87–91.

Kanehisa, M., Goto, S., Sato, Y., Furumichi, M., and Tanabe, M. (2012) KEGG for integration and interpretation of large-scale molecular data sets. *Nucleic Acids Res* **40:** D109–D114.

Kanoksilapatham, W., Gonzalez, J., and Robb, F. (2007) Directed-mutagenesis and deletion generated through an improved overlapping-extension PCR based procedure. *Silpakorn U Science & Tech J* **1:** 7–12.

Kanungpean, D., Kakuda, T., and Takai, S. (2011) Participation of CheR and CheB in the chemosensory response of Campylobacter jejuni. *Microbiology* **157:** 1279–1289.

Karimova, G., Pidoux, J., Ullmann, A., and Ladant, D. (1998) A bacterial two-hybrid system based on a reconstituted signal transduction pathway. *Proc Natl Acad Sci USA* **95:** 5752–5756.

Kazmierczak, M.J., Wiedmann, M., and Boor, K.J. (2005) Alternative sigma factors and their roles in bacterial virulence. *Microbiol Mol Biol Rev* **69:** 527–543.

Kirby, J.R. (2009) Chemotaxis-like regulatory systems: unique roles in diverse bacteria. *Annu Rev Microbiol* **63:** 45–59.

Kirby, J.R., and Zusman, D.R. (2003) Chemosensory regulation of developmental gene expression in *Myxococcus xanthus. Proc Natl Acad Sci USA* **100:** 2008–2013.

Larkin, M.A., Blackshields, G., Brown, N.P., Chenna, R., McGettigan, P.A., McWilliam, H., *et al.* (2007) Clustal W and Clustal X version 2.0. *Bioinformatics* **23:** 2947–2948.

Le Moual, H., and Koshland, J.D.E. (1996) Molecular evolution of the c-terminal cytoplasmic domain of a superfamily of bacterial receptors involved in taxis. *J Mol Biol* **261:** 568–585.

Martin, A.C., Wadhams, G.H., Shah, D.S.H., Porter, S.L., Mantotta, J.C., Craig, T.J., *et al.* (2001) CheR- and CheB-dependent chemosensory adaptation system of rhodobacter sphaeroides. *J Bacteriol* **183:** 7135–7144.

Mihaljevic, R.R., Sikic, M., Klancnik, A., Brumini, G., Mozina, S.S., and Abram, M. (2007) Environmental stress factors affecting survival and virulence of Campylobacter jejuni. *Microb Pathog* **43:** 120–125.

Missiakas, D., and Raina, S. (1998) The extracytoplasmic function sigma factors: role and regulation. *Mol Microbiol* **28:** 1059–1066.

Nowlin, D.M., Bollinger, J., and Hazelbauer, G.L. (1987) Sites of covalent modification in Trg, a sensory transducer of *Escherichia coli. J Biol Chem* **262:** 6039–6045.

Nowlin, D.M., Bollinger, J., and Hazelbauer, G.L. (1988) Site-directed mutations altering methyl-accepting residues of a sensory transducer protein. *Proteins* **3:** 102–112.

Park, C., Dutton, D.P., and Hazelbauer, G.L. (1990) Effects of glutamines and glutamates at sites of covalent modification of a methyl-accepting transducer. *J Bacteriol* **172:** 7179–7187.

Parkinson, J.S. (2010) Signaling mechanisms of HAMP domains in chemoreceptors and sensor kinases. *Annu Rev Microbiol* **64:** 101–122.

Perez, E., Zheng, H., and Stock, A.M. (2006) Identification of methylation sites in thermotoga maritima chemotaxis receptors. *J Bacteriol* **188:** 4093–4100.

Price, C.W. (2002) General stress response. In *Bacillus Subtilis and Its Closest Relatives: From Genes to Cells*. Sonenshein, A.L., Hoch, J.A., and Losick, R. (eds). Washington, DC, USA: ASM Press, pp. 369–384.

Punta, M., Coggill, P.C., Eberhardt, R.Y., Mistry, J., Tate, J., Boursnell, C., *et al.* (2012) The Pfam protein families database. *Nucleic Acids Res* **40:** D290–D301.

van Schaik, W., Tempelaars, M.H., Wouters, J.A., de Vos, W.M., and Abee, T. (2004) The Alternative sigma factor σB of *Bacillus cereus*: response to stress and role in heat adaptation. *J Bacteriol* **186:** 316–325.

van Schaik, W., Tempelaars, M.H., Zwietering, M.H., de Vos, W.M., and Abee, T. (2005) Analysis of the role of RsbV, RsbW, and RsbY in regulating σ^B activity in *Bacillus cereus*. *J Bacteriol* **187:** 5846–5851.

Schoeni, J.L., and Wong, A.C. (2005) *Bacillus cereus* food poisoning and its toxins. *J Food Prot* **68:** 636–648.

Scott, A.E., Simon, E., Park, S.K., Andrews, P., and Zusman, D.R. (2008) Site-specific receptor methylation of FrzCD in *Myxococcus xanthus* is controlled by a tetra-trico peptide repeat (TPR) containing regulatory domain of the FrzF methyltransferase. *Mol Microbiol* **69:** 724–735.

Shapiro, M.J., and Koshland, D.E. (1994) Mutagenic studies of the interaction between the aspartate receptor and methyltransferase from *Escherichia coli*. *J Biol Chem* **269:** 11054–11059.

Stock, A.M., Robinson, V.L., and Goudreau, P.N. (2000) Two-component signal transduction. *Annu Rev Biochem* **69:** 183–215.

Surette, M.G., and Stock, J.B. (1996) Role of α-helical coiled-coil interactions in receptor dimerization, signaling, and adaptation during bacterial chemotaxis. *J Biol Chem* **271:** 17966–17973.

Terwilliger, T.C., Wang, J.Y., and Koshland, D.E. (1986) Surface structure recognized for covalent modification of the aspartate receptor in chemotaxis. *Proc Natl Acad Sci USA* **83:** 6707–6710.

Thomas, S.A., Brewster, J.A., and Bourret, R.B. (2008) Two variable active site residues modulate response regulator phosphoryl group stability. *Mol Microbiol* **69:** 453–465.

Tran, H., Krushkal, J., Antommattei, F., Lovley, D., and Weis, R. (2008) Comparative genomics of Geobacter chemotaxis genes reveals diverse signaling function. *BMC Genomics* **9:** 471.

Voelker, U., Voelker, A., and Haldenwang, W.G. (1996) Reactivation of the *Bacillus subtilis* anti-sigma B antagonist, RsbV, by stress- or starvation-induced phosphatase activities. *J Bacteriol* **178:** 5456–5463.

Wadhams, G.H., and Armitage, J.P. (2004) Making sense of it all: bacterial chemotaxis. *Nat Rev Mol Cell Biol* **5:** 1024–1037.

Wang, S.W., Chen, C.Y., Tseng, J.T., Liang, S.H., Chen, S.C., Hsieh, C., *et al.* (2009) orf4 of the *Bacillus cereus* sigB gene cluster encodes a general stress-inducible Dps-like bacterioferritin. *J Bacteriol* **191:** 4522–4533.

Wise, A.A., Fang, F., Lin, Y.-H., He, F., Lynn, D.G., and Binns, A.N. (2010) The receiver domain of hybrid histidine kinase VirA: an enhancing factor for vir gene expression in *Agrobacterium tumefaciens*. *J Bacteriol* **192:** 1534–1542.

Zotta, T., Ricciardi, A., Ciocia, F., Rossano, R., and Parente, E. (2008) Diversity of stress responses in dairy thermophilic streptococci. *Int J Food Microbiol* **124:** 34–42.

Supporting information

Additional Supporting Information may be found in the online version of this article:

Fig. S1. Conservation of potential methylation sites among RsbK family members.
A. Multiple sequence alignment of the sequence segment containing potential methylation sites of 79 RsbK orthologue. The alignment score for each aligned residue column were displayed as histogram in below. Position of the two heptad segments involved in σ^B regulation are marked by a black solid line and a grey double line respectively.
B. Sequence signature of the two successive heptad containing potentially methylated residue Glu^439 and Glu^446. As indicated in the msa score histogram, these two heptads are high score aligned block. Logo text colour scheme are used to indicate the biochemical property of residues.
Table S1. Bacterial strains and plasmids.
Table S2. Oligonucleotides used in this study.
Table S3. Summary of RsbK family on the basis of sequence homology and gene organization.

Please note: Wiley-Blackwell are not responsible for the content or functionality of any supporting materials supplied by the authors. Any queries (other than missing material) should be directed to the corresponding author for the article.